Biomaterials 31 (2010) 2272–2277

Contents lists available at ScienceDirect

Biomaterials

journal homepage: www.elsevier.com/locate/biomaterials

Bioconjugation of barium titanate nanocrystals with immunoglobulin G antibody for second harmonic radiation imaging probes

Chia-Lung Hsieh [a,b,*], Rachel Grange [a], Ye Pu [a], Demetri Psaltis [a]

[a] School of Engineering, EPFL, Station 17, 1015 Lausanne, Switzerland
[b] Department of Electrical Engineering, California Institute of Technology, 1200 East California Boulevard, MC 136-93, Pasadena, CA 91125, USA

ARTICLE INFO

Article history:
Received 9 November 2009
Accepted 26 November 2009
Available online 8 December 2009

Keywords:
Confocal microscopy
Cross-linking
Immunochemistry
In vitro test
Nanoparticle
Surface modification

ABSTRACT

The second harmonic generation (SHG) active nanocrystals have been demonstrated as attractive imaging probes in nonlinear microscopy due to their coherent, non-bleaching and non-blinking signals with a broad flexibility in the choice of excitation wavelength. For the use of these nanocrystals as biomarkers, it is essential to prepare a chemical interface for specific labeling. We developed a specific labeling scheme for barium titanate ($BaTiO_3$) nanocrystals which we use as second harmonic radiation imaging probes. The specificity was achieved by covalently coupling antibodies onto the nanocrystals. We demonstrate highly specific labeling of the nanocrystal conjugates in an antibody microarray and also the membrane proteins of live biological cells in vitro. The development of surface functionalization and bioconjugation of SHG active nanocrystals provides the opportunities of applying them to biological studies.

© 2009 Elsevier Ltd. All rights reserved.

1. Introduction

Detecting and tracing specific molecules of interest are important for studying the function and the behavior of biological systems. Biomarkers have been developed to achieve this goal by creating a contrast between signal and background. An extremely effective method to obtain such contrast is to shift the radiated signal away from the excitation wavelength so that the excitation can be efficiently removed by optical filters. Several mechanisms of converting the wavelength have been demonstrated, such as single-photon and multi-photon fluorescence [1–5], endogenous SHG [6–10], and third harmonic generation (THG) [7,11–13]. Among them, fluorescent biomarkers such as green fluorescent proteins (GFPs) [1], organic dyes [2], and quantum dots (QDs) [4] have been widely used for biomedical imaging due to their excellent brightness and biocompatibility.

We have developed $BaTiO_3$ nanocrystals [14,15] as biomarkers using the SHG signal from nanoparticles [16–30]. We refer to these probes as "Second Harmonic Radiation IMaging Probes (SHRIMPs)". When a nanocrystal of non-centrosymmetric structure is optically excited at a fundamental frequency, it emits the optical signal at the exact doubled frequency. Materials with crystalline structure lacking a center of symmetry are capable of efficient SHG, while centrosymmetric materials have a weak SHG response mostly from the surface where the symmetry is broken [31]. Thus, when imaged at the second harmonic frequency, SHRIMPs provide an effective contrast mechanism between the markers and the generally unstructured or isotropic biological environment. Ordered and highly polarizable biological non-centrosymmetric structures, such as collagen fibers, have endogenous SHG [6–10]. However, in most biological cell components, the endogenous SHG from the cell interface layers is weak [32].

Unlike fluorescence, the SHG process only involves virtual electron energy transition without nonradiative energy loss. Owing to this virtual transition process, SHRIMPs do not bleach over time and emit a stable, non-blinking signal that does not saturate with increasing excitation power. Furthermore, the response time of SHG process is in the femtosecond scale, which is four to five orders of magnitude faster than typical fluorophores. This allows for the observation of fast dynamic processes over a long time. In addition, SHG is generally a non-resonant process which offers broad flexibility in the choice of excitation wavelength. The coherent nature of the SHG signal is also a major advantage, providing a possibility to detect the second harmonic signal generated from the nanocrystals with interferometric optical techniques [14,15,18].

The SHG properties of several kinds of nanocrystals have been recently reported: $BaTiO_3$ [14,15,25], ZnO [16,23,26], $KTiOPO_4$ (KTP) [18,22,24,27], $Fe(IO_3)_3$ [20,30], $KNbO_3$ [21], $Sr_{0.6}Ba_{0.4}Nb_2O_6$ [28], organic nanocrystals [17], and SHG active crystalline

* Corresponding author at: School of Engineering, EPFL, Station 17, 1015 Lausanne, Switzerland.
E-mail address: chia-lung.hsieh@epfl.ch (C.-L. Hsieh).

0142-9612/$ – see front matter © 2009 Elsevier Ltd. All rights reserved.
doi:10.1016/j.biomaterials.2009.11.096

organic-inorganic hybrid nanoparticles [19,29]. In our previous work, we have characterized the SHG response from individual $BaTiO_3$ nanocrystals and also used them as SHRIMPs for non-specific cell labeling [15]. For most biological applications, it is essential to prepare a chemical interface for specific labeling. The surface functionalization of these SHG active dielectric nanomaterials can be limited by lack of compatibility between the inorganic nanoparticles and the organic bio-molecules. It has been reported that SHG and sum-frequency-generation active ZnO nanocrystals can be stabilized in aqueous suspension and further incorporated with the folic acid molecules for tumor cell targeting when being encapsulated in phospholipid micelles [23]. In this paper, we demonstrate the specific labeling of $BaTiO_3$ nanocrystals by directly conjugating immunoglobulin G (IgG) antibody on the surface of the nanocrystals. To the best of our knowledge, this is the first demonstration of functionalized SHG nanocrystals by covalently coupling the antibody to the surface of the nanocrystals. The antibody conjugation provides a flexible scheme to target a specific molecule in a biological specimen.

2. Experimental section

2.1. Materials

$BaTiO_3$ nanocrystals in dry powder were commercially available from Tech-Powder (TechPowder S.A. Lausanne, Switzerland). Nitric acid (65%) and ammonia (25%) were purchased from AnalaR Normapur, VWR. 3-aminopropyltriethoxysilane (APTES, >98%), ethylenediaminetetraacetic acid (EDTA, >99.99%), 2-mercaptoethanol (>98%), DL-dithiothreitol (DTT, 1M), bovine serum albumin (BSA, >98%), Tween 20, and Gelatin were purchased from Sigma–Aldrich. Ethanol (>99.8%) was obtained from Fluka. Sulfosuccinimidyl 4-[*N*-maleimidomethyl]cyclohexane-1-carboxylate (sulfo-SMCC) was obtained from Thermo Scientific. 2-(N-morpholino)ethanesulfonic acid (MES, 0.5 M) was purchased from Biochemika Ultra. The exchange buffer was composed of 50 mM of MES and 2 mM of EDTA in distilled water pH 7. Phosphate-buffered salines (PBS pH 7.4), Dulbecco's Modified Eagle Medium with high glucose (DMEM), fetal bovine serum (FBS), and Calcein AM (C3100MP) were obtained from Invitrogen. Four types of primary antibodies used in this work were Mouse anti-Human IgG (CD144, VE-caderin, BD Biosciences), Goat anti-Human IgG (Jackson ImmunoResearch), Rabbit anti-Human IgG (Jackson ImmunoResearch), and Mouse monoclonal antibody specific to human HLA class I antigens (MHBC01, Invitrogen). The secondary antibody was a Donkey anti-Mouse IgG antibody-Cy5 (Jackson ImmunoResearch).

2.2. Antibody microarray preparation

Three different types of the primary antibodies and also the buffer solution were printed separately and repeatedly on the slide in the form of a microarray. The three types of the primary antibodies were Mouse anti-Human IgG (CD144), Goat anti-Human IgG, and Rabbit anti-Human IgG. The Mouse anti-Human IgG was the target primary antibody because the secondary antibody was an anti-Mouse IgG. The primary antibodies were printed on the aldehydesilane coated slides (Nexterion Slide AL, Schott Nexterion) by a contact-printing robotic microarrayer (OmniGrid 300, Genomic Solutions) equipped with SMP2 pins (TeleChem International) at 22 °C with 60% relative humidity. The spotting buffer solution was PBS with 5% glycerol, and the concentration of the primary antibody was 0.2 mg/mL. The size of the printing spot is 90 μm in diameter and the period between two adjacent spots is 200 μm. After printed, the slides were incubated for an hour at 22 °C at 75% relative humidity. During the incubation, the proteins cross-linked to the slide. Then the free aldehyde groups on the slides were blocked by 50 mM triethanolamine (titrated to pH 8 with boric acid) for 30 min at room temperature. The slide was rinsed by water and then dried by centrifugation.

2.3. HeLa cell culture and immunostaining

HeLa cell line was provided by the Biomolecular Screening Facility at EPFL, Switzerland. The HeLa cells were grown in flasks containing the growth media (DMEM supplemented with 10% heat-inactivated FBS) at 37 °C in a humidified atmosphere of 5% CO_2. The HeLa cells were harvested from the flask by applying Trypsin for 4 min at 37 °C. We counted and prepared 10^6 of cells for each immunostaining. The cells were washed and suspended in 2 mg/mL of BSA in PBS. We blocked the cells with 2 mg/mL of BSA in PBS for 1 h at room temperature to reduce the non-specific labeling. The primary antibody (Mouse monoclonal antibody specific to human HLA class I antigens) was introduced at a dilution of 1:100 and incubated with the cells for 1 h at room temperature. The cells were then washed three times with 2 mg/mL of BSA in PBS by centrifugation to remove the unconjugated primary antibodies. The primary-antibody-labeled cells were then mixed with the secondary-antibody-SHRIMP conjugates at a concentration of about 10^9 nanoparticles/mL at room temperature for 1 h. The cells were then washed three times with 2 mg/mL of BSA in PBS. Finally the cells were placed in a petri dish filled with growth media to allow the cell to attach for imaging. The cells were further stained with Calcein AM for fluorescent imaging.

2.4. SHG wide-field microscope

We used a SHG wide-field microscope to characterize the SHG properties from $BaTiO_3$ nanocrystals. The excitation was a linearly polarized Ti:sapphire oscillator (150 fs pulse duration centered at 800 nm wavelength with a 76 MHz repetition rate). The laser beam was slightly focused by a lens of 5-cm focal length to reach the peak intensity of 1 GW/cm^2 on the sample. The SHG signal was collected by a 100 × 1.4 numerical aperture (NA) oil-immersion objective (UPLSAPO 100XO, Olympus) in the forward direction and imaged directly on an electron multiplying charge coupled device (EMCCD, Andor iXonEM+ 885) with a lens of 20-cm focal length. The excitation was removed by using narrow band-pass filters centered at 400 nm.

2.5. Scanning confocal microscope

A standard scanning confocal microscope (Leica, SP5) was used to image the cells labeled by SHRIMPs. The excitation light source consisted of linearly polarized femtosecond laser pulses (Coherent, Chameleon) and the excitation wavelength was centered at 812 nm wavelength. The laser was focused by a 20 × 1.0 NA water-immersion microscope objective. The SHG signal and two-photon fluorescence were collected in epi-geometry simultaneously with two independent channels: SHG channel (400–415 nm) and fluorescent channel (500–550 nm). The transmission signal at the fundamental wavelength is also detected as the third channel.

3. Results and discussion

3.1. Characterization of $BaTiO_3$ nanocrystals

We started with $BaTiO_3$ nanocrystals in dry powder. X-ray diffraction data (not shown here) confirms that the crystal structure is tetragonal, which is non-centrosymmetric, allowing for efficient SHG without any further treatment. A bright-field transmission electron microscope (TEM) image of $BaTiO_3$ nanocrystals is shown in Fig. 1. The nanocrystals are nearly spherical in shape and between 60 nm and 110 nm in diameter. The $BaTiO_3$ nanocrystals were dispersed in water and treated with ultrasound (Branson digital sonifier 450) to break them into individual nanocrystals.

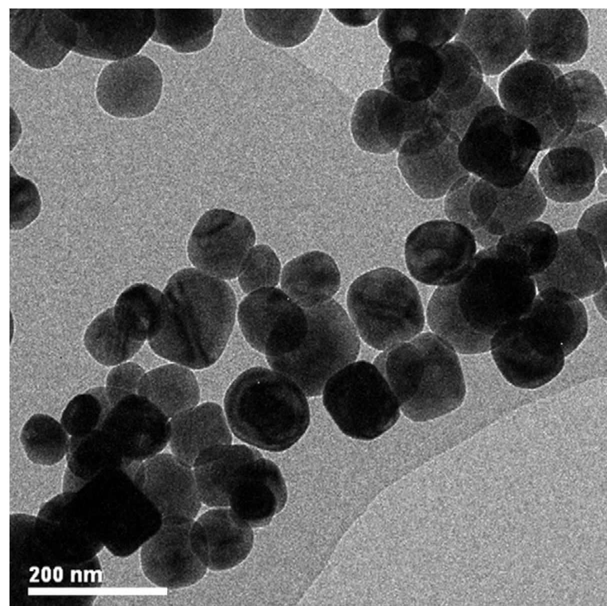

Fig. 1. Bright-field TEM image of $BaTiO_3$ nanocrystals.

Download English Version:

https://daneshyari.com/en/article/8682

Download Persian Version:

https://daneshyari.com/article/8682

Daneshyari.com